jmr&t
Journal of Materials Research and Technology
www.jmrt.com.br

Original Article

Enhancing microstructure and durability of concrete from ground granulated blast furnace slag and metakaolin as cement replacement materials

Ping Duan[a,*], *Zhonghe Shui*[a], *Wei Chen*[a], *Chunhua Shen*[b]

[a]*Wuhan University of Technology, State Key Laboratory of Silicate Materials for Architectures, Wuhan, China*
[b]*Wuhan University of Technology, Center of Materials Research and Analysis, Wuhan, China*

ARTICLE INFO

Article history:
Received 8 October 2012
Accepted 21 November 2012

Keywords:
Pore structure
Interfacial transition zone
Metakaolin
Ground granulated blast furnace slag
Durability

ABSTRACT

Recycling of industrial wastes and by-products can help reduce the cost of waste treatment prior to disposal and eventually preserve natural resources and energy. In this work, the pore structure and interfacial transition zone (ITZ) of concrete incorporating ground granulated blast furnace slag (GGBS) and metakaolin (MK) were analyzed. Some techniques including mercury intrusion porosimetry (MIP), microhardness tester and scanning electronic microscopy (SEM) were employed to characterize the effects of GGBS and MK on the pore structure, microhardness and morphology of ITZ at 28 days. The compressive strength and durability including carbonation resistance, chloride penetration resistance and freeze-thaw resistance were experimental evaluated in relation to their pore characters and ITZ. Meanwhile, the influence of silicon, as the major component of GGBS and MK, on thermodynamic stability of hydrate phases was further investigated. The experimental results show that GGBS and MK have positive impact on pore refinement and ITZ enhancement of concrete. The development of the compressive strength and durability is closely related to the evolution of the pore structure and ITZ. Thermodynamic stability analysis indicates that silicon, as the major component of GGBS and MK, influences the stability of hydrate phases according to changes in Gibbs free energy of reaction.

1. Introduction

Pore structure of concrete includes air voids, capillary pores and gel pores. As one of the important characters of concrete materials, pore structure possesses a definite proportion in concrete and it has important implications on transmission characteristics [1,2]. Specifically, pore structure parameters including the porosity and pore size distribution are important components of microstructure. Research conducted before indicated that pore structure affects permeability, frost resistance and physical mechanical performance of concrete [3-5].

The traditional picture of the ITZ in concrete involves an approximately 30-50 μm zone around each aggregate, within which the porosity increases as the aggregate interface is

*Corresponding author.
E-mail address: dp19851128@sina.com (P. Duan).

2238-7854
http://dx.doi.org/10.1016/j.jmrt.2013.03.010

approached. Crystal enrichment and orientation of $Ca(OH)_2$ are the main reasons for the weak interface, it indirectly reflects the pore structure and compact degree [6-8]. Different mineral admixtures strongly affect the microstructure in ITZ.

It produces a large amount of greenhouse gas emissions, mostly CO_2, resulting from release of CO_2 from limestone in the pyro-processing of clinker. On the other hand, the concrete industry is one of the major consumers of natural resources. In order to reduce energy consumption, CO_2 emission and increase production, cement plants produce blended cements, comprised of supplementary cementitious materials such as metakaolin [9-11], silica fume, natural pozzolan, fly ash and limestone. Meanwhile, it is a very practical fact that serious environmental conditions can influence the formation of concrete microstructure and deteriorate the concrete structure. In order to improve the performance of concrete capable of withstanding serious environmental conditions, supplementary cementitious materials include industrial by-products such as slag, fly ash, silica fume, etc. as well as natural materials such as ground limestone and metakaolin are also widely used. Each of these materials has a unique but distinctive effect on the performance of concrete. Some stable products maybe form due to pozzolanic reactions between these mineral admixtures and cement hydration product $Ca(OH)_2$ to improve the microstructure development.

The complexity of supplementary cementitious materials in blended cements system has meant that results are often confined to measurement of a few of the many parameters affecting performance under controlled conditions. However, thermodynamics provides a consistent framework for the analysis of complex systems. Geochemists, faced by similar problems of treating complex systems, have developed and validated computer codes capable of being implemented on a PC. Many reliable code packages are available in the public domain. Furthermore codes can be coupled to fluid mass transport modeling modules; in this case, thermodynamic datasets supply important physical properties.

Surveys conducted before [12-16] mainly focuses on characterizing single characteristics of concrete materials with single test technology, and very little work has been carried out on contrast between different test technologies or evolution of the microstructure and durability of concrete incorporating various mineral admixtures including ground granulated blast furnace slag and metakaolin. This paper presents the results of a study on effects of ground granulated blast furnace slag and metakaolin on pore structure, ITZ, compressive strength and durability aspects of concrete and thermodynamic stability of hydrate phases.

Table 1 – The properties of cement.

Compressive strength (MPa)		Flexural strength (MPa)		Initial setting time (min)	Final setting time (min)
3 days	28 days	3 days	28 days		
34.3	60.5	6.3	8.7	132	187

2. Experimental

2.1. Materials and mix design

Portland cement (CEM I 42.5) (relative density 3,100 kg/m^3, specific surface area 369.6 m^2/kg) was used as binder in the study. The properties of cement is shown in Table 1. Mineral admixtures were ground granulated blast furnace slag (relative density 2900 kg/m^3) and metakaolin (relative density 2600 kg/m^3) obtained from the slow calcination of kaolinite at 750 °C. Their chemical compositions are shown in Table 2. Natural crushed limestone with maximum size of 25 mm was used as coarse aggregate and natural river sand with fineness modulus of 2.8 was used as fine aggregate for production of all concretes. In addition, polycarboxylates superplasticizer (density 1.08 g/mL, solid content 20%) was used to attain the required workability. Four concrete mixtures were cast with different cement replacement levels (by mass) of MK and GGBS. Mix proportion is shown in Table 3.

Table 2 – Chemical composition of Portland cement and mineral admixtures (%).

	SiO_2	Fe_2O_3	Al_2O_3	CaO	MgO	SO_3	LOI
Cement	21.35	3.31	4.67	62.60	3.08	2.25	0.95
Slag	34.26	1.23	17.11	35.17	6.41	1.72	0.15
Metakaolin	50.27	0.75	34.46	0.29	–	0.21	0.06

LOI: loss on ignition.

Table 3 – Mix proportion of concrete (kg/m^3).

	Cement	Slag	Metakaolin	Water	Fine aggregate	Coarse aggregate
O	360	0	0	180	681	1160
GGBS	324	36	0	180	681	1160
MK	324	0	36	180	681	1160
GGBS+MK	288	36	36	180	681	1160

GGBS: ground granulated blast furnace slag; MK: metakaolin.

Four kinds of specimens for the compressive strength test with the size of 150 mm × 150 mm × 150 mm are: O-reference ordinary concrete, GGBS-concrete with slag, MK-concrete with metakaolin and GGBS+MK-concrete with ground granulated blast furnace slag and metakaolin.

2.2. Casting and curing

Cubic specimens (150 mm × 150 mm × 150 mm), cylindrical specimens (Φ100 mm × 200 mm) and prism specimens (100 mm × 100 mm × 400 mm) were cast for various tests including compressive strength test, MIP test, microhardness test, carbonation test, chloride ion penetration test and freeze-thaw test. The specimens were demoulded and stored in a curing room at 20 ± 2 °C and 90 ± 5% RH until the age of tests.

2.3. Test procedures

2.3.1. Compressive strength test

Compressive strength test was carried out on 150 mm × 150 mm × × 150 mm cubic specimens at the ages of 3, 28 and 180 days using a 2,000 kN capacity compression testing machine. The compressive strength value was the average of three specimens.

2.3.2. Mercury intrusion porosimetry

The porosity and pore size distribution were measured by MIP (Micromeritics AutoPore IV 9510 mercury intrusion porosimeter) with a maximum pressure of 207 MPa. The contact angle was 140° and the measurable pore size ranged from about 6 nm to 360 μm. Mercury surface tension assumed for tests was 485.0 dyn/cm. The Washburn equation was used to calculate the pore radius. The samples in the shape of pellets of about 5 mm in size without coarse aggregate for pore structure testing were separated from the crushed specimens used. The samples were immerged in ethanol to avoid rehydration immediately after being crushed and dried at about 105 °C for 24 hours before MIP test.

2.3.3. Measurement of microhardness

Microhardness tester was used to investigate the interface between aggregates and cement matrix. The specimens for ITZ microhardness test were cut into slices with the size of 100 mm × 100 mm × 10 mm. Slices cut from the middle of the cubic sample, containing the ITZ between aggregate and mortar, were polished with # 600 abrasive paper and then # 1,500 abrasive paper to obtain an adequately smooth surface with a minimum of damage. Slices were then carefully sealed to avoid carbonation, which might lead to larger measured hardness values because of the carbonation product ($CaCO_3$). To avoid overlapping of press mark of measuring points, advanced measuring method was employed as shown in Fig. 1.

2.3.4. Micrographs test

The micrographs of ITZ between aggregate and cement matrix were obtained by means of JSM-5610LV scanning electronic microscopy (SEM). The specimens for ITZ morphology observation were cut into prisms with size of 8 mm × 8 mm × 6 mm.

2.3.5. Carbonation test

Concrete specimens with the size of 100 mm × 100 mm × × 400 mm were used for carbonation property test. After cured in standard curing conditions (RH ≥ 90%; T = 20 ± 3 °C) for specific days, specimens were dried at 60 °C for 48 hours. Four surface sides of specimens were sealed by wax except two opposite end sides, and then specimens were moved into carbonation chamber (RH = 70 ± 5%, T = 20 ± 3 °C, C_{CO2} = 20 ± 3%). The carbonation depth of the specimen was measured at 3, 28 and 180 days using vernier caliper after fracture surface of concrete was sprayed with phenolphthalein test solution.

2.3.6. Chloride penetrability

The chloride penetration of concrete was characterized by rapid chloride migration (RCM) test. All surfaces of the concrete specimens (50 mm thick, 100 mm diameter) except top and bottom sides were sealed by epoxy resin so that the chloride penetration can occur only in one-direction. The samples were then vacuum saturated in water as per ASTM C1202-12 [17] (3 hours in vacuum dry, water admitted under vacuum and maintained for 1 hour, followed by immersion in water at atmospheric pressure for 18 hours). At 3, 28 and 180 days of age, they were sealed in plastic containers with the test face exposed to 1.0 mol/L NaCl solution at 23 °C.

2.3.7. Freeze-thaw tests

Tests of concrete specimens (100 mm × 100 mm × 400 mm) subjected to freeze-thaw cycling were carried out in accordance with ASTM C666A [18]. The freeze-thaw tests, in which temperature varied between +20 °C and –20 °C, were performed with deionized water as the freezing liquid in which no additional salts were dissolved. In the tests, the losses of both the relative dynamic modulus of elasticity and the weight

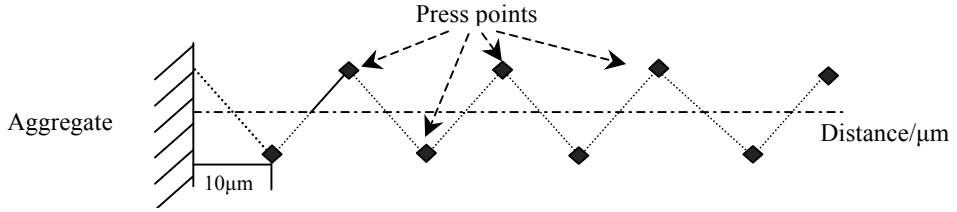

Fig. 1 – Distribution of measuring points.

in the concrete specimens were measured and recorded. Three specimens were tested for each concrete mix. The test specimens are shown in Fig. 2.

2.3.8. Chemical thermodynamic modelling

Thermodynamic modeling was used to calculate the composition of the stable hydrate assemblage and of the surrounding solution assuming thermodynamic equilibrium. GEMS (Gibbs free energy minimization) is a broad-purpose geochemical modeling code which uses Gibbs energy minimization and computes equilibrium phase assemblage and speciation in a complex chemical system from its total bulk elemental composition. Chemical interactions involving solids, solid solutions, and aqueous electrolyte are considered simultaneously. Thermodynamic data for aqueous species as well as for many solids are taken from the PSI thermodynamic dataset, which has been adapted for the use in GEMS.

3. Results and discussion

3.1. Effects of mineral admixtures on pore structure of concrete

Effects of mineral admixtures on pore structure of concrete at 28 days are shown in Fig. 3 and Fig. 4, respectively. In Fig. 3, accumulative intrusion volume decrease gradually with the addition of GGBS, metakaolin and the compound of GGBS and metakaolin, and decreases to 94.5%, 78.5% and 70%, respectively. Critical pore diameters also decrease and the reduction is the most prominent when incorprating GGBS and metakaolin. The most probable pore diameter corresponding to the highest peak in Fig. 4 also decreases gradually, and the curve has shifted to the small pore diameter portion. Results from Fig. 3 and Fig. 4 demonstrate that with the addition of admixtures, the pore characteristics of concrete are greatly improved. Specifically, pore structure is optimized and pore size distribution is more reasonable. Minerals admixtures have positive impact on pore refinement of concrete. The improving effects when incorprating GGBS and metakaolin are the most remarkable.

Due to micro aggregates filling and pozzolanic effect of GGBS and metakaolin, the total pore volume of concrete decreases obviously, and pore size distribution has shifted to small pore diameter portion. Compacting hydration product C-S-H gel forms due to pozzolanic effect and fine particles bridge the gap between cement particles, which makes the paste denser. C-S-H gels with higher strength optimize the microstructure of concrete.

3.2. Effects of mineral admixtures on microhardness of interfacial transition zone

The results provided in Fig. 5 show effects of GGBS and MK on ITZ of concrete. With the addition of GGBS, metakaolin, and the compound of GGBS and metakaolin, microhardness of ITZ increase gradually and widths of ITZ decease remarkably. It indicates that microstructure of ITZ has been optimized by mineral admixtures. As discussed above, compacting hydration product C-S-H gel forms and content of $Ca(OH)_2$ decreases due to pozzolanic effect. Fine particles bridge the gap between cement paste and aggregate, which makes the concrete denser. Therefore, the microstructures of concrete are highly optimized.

Fig. 2 – Freeze-thaw tests of concrete specimens.

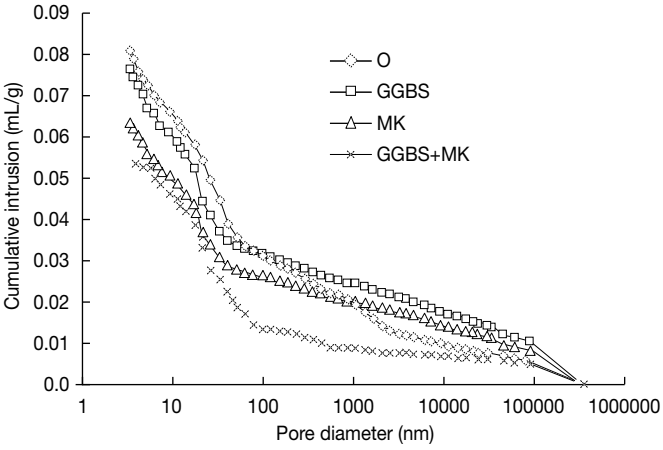

Fig. 3 – Cumulative intrusion volume of concrete. GGBS: ground granulated blast furnace slag; MK: metakaolin.

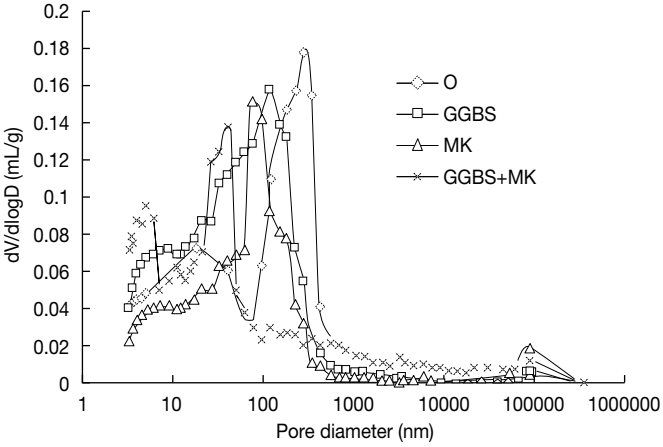

Fig. 4 – Incremental intrusion volume of concrete. GGBS: ground granulated blast furnace slag; MK: metakaolin.

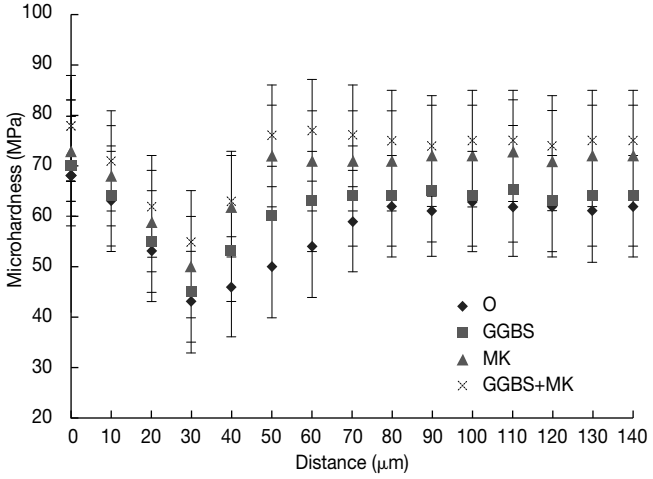

Fig. 5 – Effects of mineral admixtures on interfacial transition zone of concrete.

3.3. Micro-morphology of interfacial transition zone

Micro-morphology of ITZ of concrete are observed and shown in Fig. 6. The ITZ morphology varies with different mineral admixtures.

In Fig. 6a, more amorphous C-S-H gels mix with needle-like ettringite and CH crystals, expansive destruction from hydration products result in looser structure and micro-cracks. As shown in Fig. 6b, c and d, with addition of mineral admixtures, composition of ITZ changes. Specifically, compacting hydration product C-S-H gel forms and content of $Ca(OH)_2$ decreases due to pozzolanic effect. Additionally, microstructure becomes denser and micro-cracks decrease, connection between paste and aggregate is enhanced.

3.4. Compressive strength

Compressive strength results are shown in Fig. 7. In Fig. 7, with the addition of mineral admixtures, compressive strength of concrete increase gradually. With replacement of cement by admixtures, content of hydration product $Ca(OH)_2$ decreases. Meanwhile, fine particles of mineral admixture bridge the gap between cement particles, which makes the concrete denser. Combining effects improve the compressive strength development.

Results from MIP, SEM and mechanical performance indicate that pore size distribution has obvious effect on compressive strength of concrete and macro-properties of concrete material are closely related to its microstructure. The results can also be obtained in later durability aspects tests.

3.5. Carbonation depth

The results of carbonation depth of concrete are shown in Fig. 8. With the addition of GGBS and metakaolin, carbonation depth of concrete decreases gradually. This phenomenon was mainly due to pozzolanic reactivity of mineral admixtures. With replacement of cement by GGBS and metakaolin, content of hydration product $Ca(OH)_2$ decreases. Meanwhile, fine particles of metakaolin bridge the gap between cement particles, which makes the concrete denser and CO_2 could

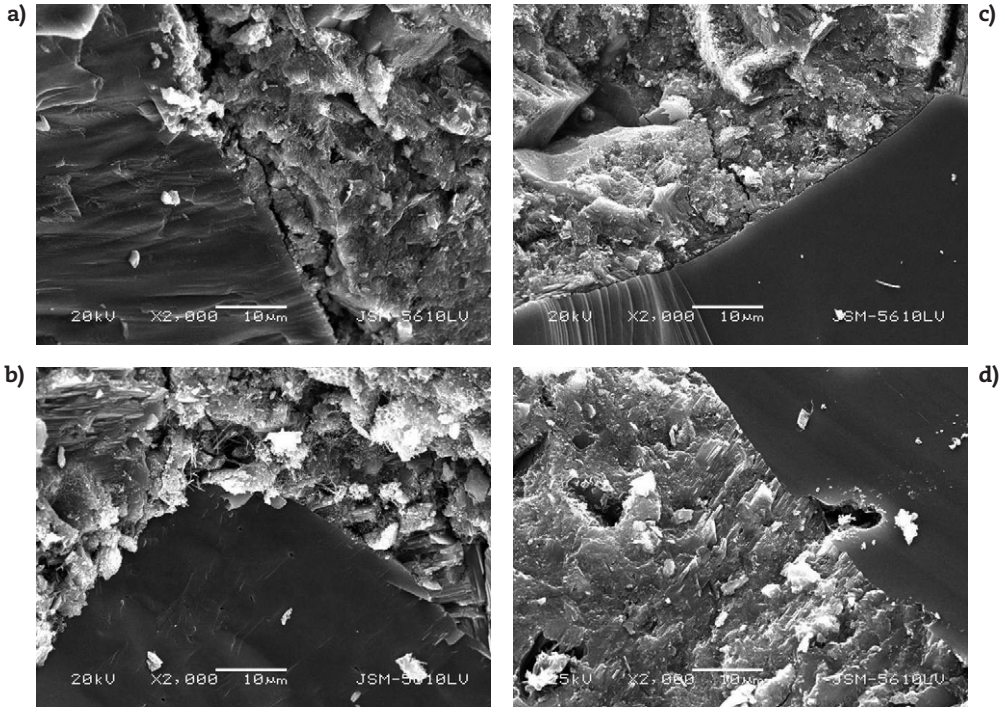

Fig. 6 – Micro-morphology of interfacial transition zone at 28 days (a) O; (b) ground granulated blast furnace slag; (c) metakaolin; (d) ground granulated blast furnace slag+ metakaolin. GGBS, ground granulated blast furnace slag; MK: metakaolin.

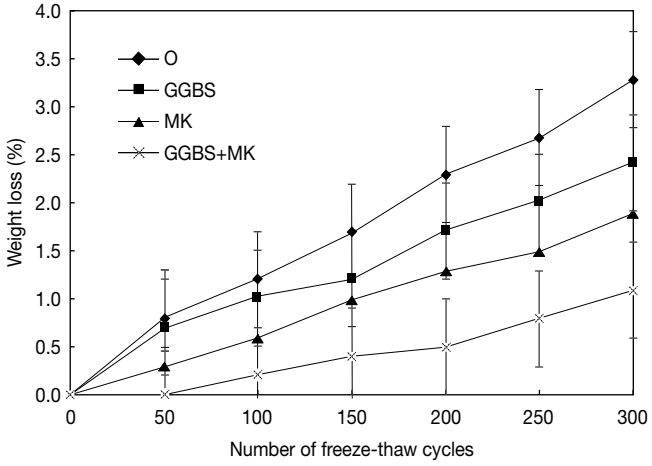

Fig. 7 – Compressive strength of concrete. GGBS: ground granulated blast furnace slag; MK: metakaolin.

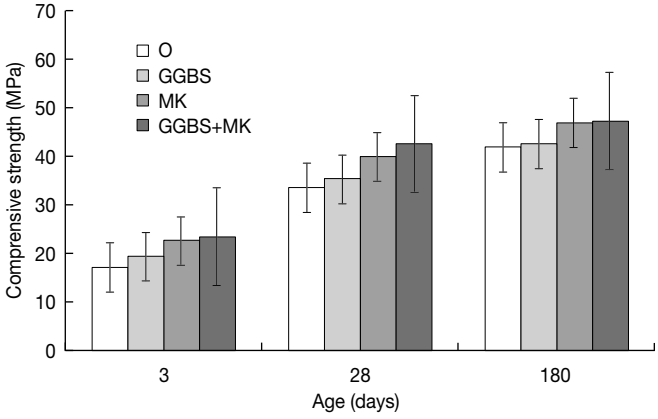

Fig. 8 – Carbonation depth of concrete. GGBS: ground granulated blast furnace slag; MK: metakaolin.

hardly enter in interconnected pores in concrete. Therefore, carbonation resistance of concrete was enhanced especially by compound of GGBS and MK.

Results from MIP, micro-morphology of ITZ and cabonation properties indicate that pore size distribution and compact degree have obvious effect on durability and macro-properties of concrete material are closely related to its microstructure.

3.6. Chloride ion penetration

Lower chloride penetration under standardized conditions indicates a denser concrete, hence a more durable concrete in terms of chloride resistance. The calculated chloride ions migration coefficients for the mixes are shown in Fig. 9. It is observed that the plain concrete specimens present higher chloride migration coefficient and it results from coarser pore structure of plain Portland cement concrete.

Both the MK and GGBS concretes showed lower chloride migration coefficients than the OPC. It should be mentioned that MK performed beneficial effect on the chloride penetration resistance especially the compound of GGBS and MK. From Fig. 9 we can see that the longer the curing age the lower the chloride migration coefficient is. It can be also seen that a 10% GGBS and 10% MK replacement in concrete resulted in a significant improvement of chloride penetration resistance.

Among all of the specimens, concrete containing GGBS and MK performed the lowest chloride ions migration coefficient at all test ages. This result is consistent with the results of MIP, micro-morphology of ITZ and the compressive strength tests and it is proved to be a promising way to improve the durability of concrete.

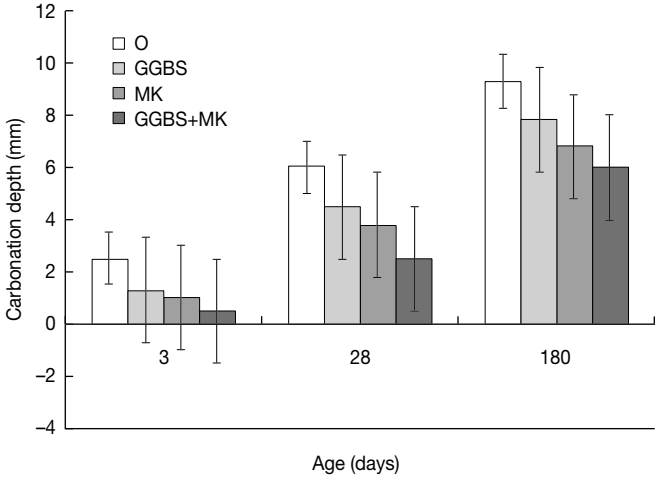

Fig. 9 – Influence of mineral admixtures on chloride ions migration coefficient. GGBS: ground granulated blast furnace slag; MK: metakaolin.

3.7. Freeze-thaw tests

In Fig. 10, weight loss decreases gradually with the addition of GGBS, metakaolin and the compound of GGBS and metakaolin, and the effect is more remarkable by GGBS and metakaolin.

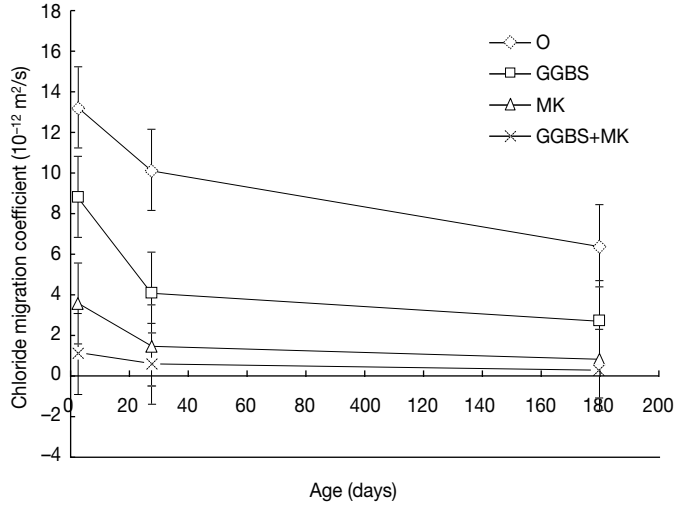

Fig. 10 – Weight losses in concrete subjected to freeze-thaw cycling in water. GGBS: ground granulated blast furnace slag; MK: metakaolin.

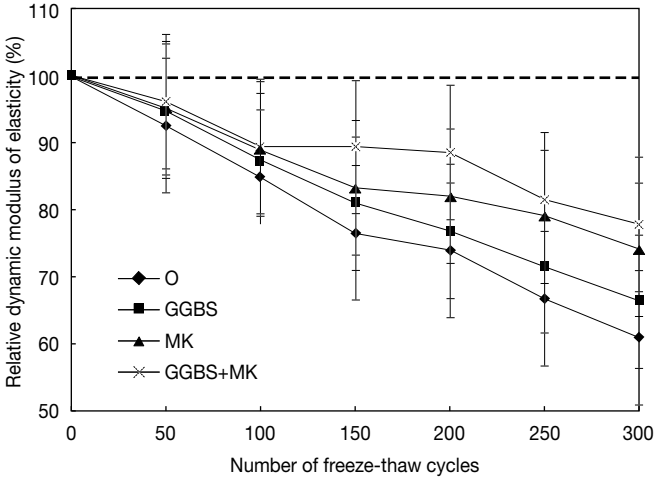

Fig. 11 – Changes in the relative dynamic modulus of elasticity of concrete subjected to freeze-thaw cycling in water. GGBS: ground granulated blast furnace slag; MK: metakaolin.

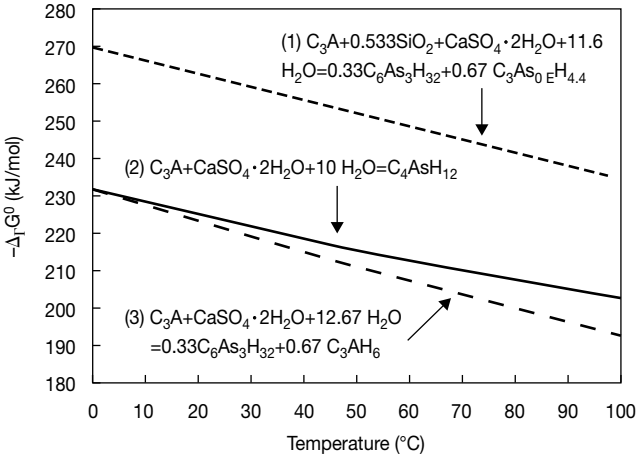

Fig.12 – Influence of mineral admixtures on the stabilities of hydrate phases.

The relative dynamic modulus of elasticity of concrete subjected to freeze-thaw cycling in water (shown in Fig. 11) also reduces gradually. Compound of GGBS and metakaolin improve freeze-thaw resistance performance remarkably.

With replacement of cement by GGBS and metakaolin, content of hydration product $Ca(OH)_2$ decreases. Meanwhile, fine particles of metakaolin bridge the gap between cement particles, which makes the concrete denser and water could hardly enter in interconnected pores in concrete. The microstructure of concrete with higher strength is denser, it reduces the content of interconnected pores, and therefore, it avoids the osmotic pressure results from migration of super cooled water and improves freeze-thaw resistance performance.

3.8. The influence of silicon on the thermodynamic stability of hydrate phases

Silicon is one of the main constituents of Portland cement. GGBS and metakaolin, which contain large amount of silica, present influence on hydration of cement. The results provided in Fig. 12 show Gibbs free energy plots of the reaction of tricalcium aluminate $3CaO\bullet Al_2O_3$ (C_3A), with gypsum and water. In the silicon-free system $CaO\text{-}Al_2O_3\text{-}CaSO_4\text{-}H_2O$, with an initial molar bulk SO_3/Al_2O_3-ratio = 1, monosulfoaluminate is more stable than the phase assemblage of ettringite (C_6AsH_{32}) and C_3AH_6 at temperatures above 5 °C (reactions (2) and (3)). But if mineral admixtures are added to the system, according to reaction (1) the phase assemblage of C_6AsH_{32} and $C_3AS_{0.8}H_{4.4}$ have a lower Gibbs free energy of reaction and is therefore thermodynamically more stable than monosulfoaluminate [reaction (2)] at temperatures from 1 to 99 °C. This aids the assumption (in item 1) that the stable hydration products C_6AsH_{32} and $C_3AS_{0.8}H_{4.4}$ form due to pozzolanic reactions between mineral admixtures and cement hydration $Ca(OH)_2$ to optimize the microstructure and enhance compressive strength of concrete.

4. Conclusions

This paper presents the results of a study on effects of ground granulated blast furnace slag and metakaolin on pore structure, ITZ, compressive strength and durability aspects of concrete and thermodynamic stability of hydrate phases.

The results and conclusions are summarized as follows:

- With the addition of GGBS and metakaolin, pore structure in concrete is optimized and pore size distribution is more reasonable, ITZ becomes denser, compressive strength of concrete increases gradually and durability aspects are enhanced. The improving effect is in the sequence: compound of metakaolin and GGBS> metakaolin >GGBS.
- There are close relationships between microstructure and durability. Concrete with higher ratio of fine porosity, reasonable pore size distribution, and higher microhardness has corresponding higher compressive strength, lower carbonation depth, lower chloride migration coefficient, lower weight loss and relative dynamic modulus of elasticity.
- In the silicon-free system $CaO\text{-}Al_2O_3\text{-}CaSO_4\text{-}H_2O$, monosulfoaluminate is more stable than the phase assemblage of ettringite (C_6AsH_{32}) and C_3AH_6 at temperatures above 5 °C. If GGBS and MK are added to the system, the phase assemblage of C_6AsH_{32} and $C_3AS_{0.8}H_{4.4}$ have a lower Gibbs free energy of reaction and is therefore thermodynamically more stable than monosulfoaluminate at temperatures from 1-99 °C.

Acknowledgements

This research has been financially supported by the National Fundamental Scientific Research Project (P R China), relevant

to 'Basic Research in Environmentally Friendly Concrete (2009CB623201)', the Youth Chenguang Project of Science and Technology of Wuhan (Project 201150431086) and the Natural Science Foundation of Hubei Province (20101j0164).

REFERENCES

[1] Frias M, Cabrera J. Pore size distribution and degree of hydration of metakaolin-cement pastes. Cem Concr Res. 2000;30:561-9.
[2] Khatib JM, Wild S. Pore size distribution of metakaolin paste. Cem Concr Res. 1996;26:1545-53.
[3] Yang CC, Chob SW, Wang LC. The relationship between pore structure and chloride diffusivity from pounding test in cement-based materials. Mater Chem Phys. 2006;100:203-10.
[4] Güneyisi E, Gesoglu M, Mermerdas K. Improving strength, drying shrinkage and pore structure of concrete using metakaolin. Mater Struct. 2008;41:937-49.
[5] Tanaka K, Kurumisawa K. Development of technique for observing pores in hardened cement paste. Cem Concr Res. 2002;32:1435-41.
[6] Asbridge AH, Page CL, Page MM. Effects of metakaolin, water/binder ratio and interfacial transition zones on the microhardness of cement mortars. Cem Concr Res. 2002;32: 1365-9.
[7] Zampini D, Shan SP. Early age microstructure of the paste-aggregate interface and it s evolution. J Mater Res. 1998;13: 1888-98.
[8] Pattanaik S, Huffman GP, Sahu S. X-ray absorption fine structure spectroscopy and X-ray diffraction study of cementitious materials derived from coal combustion by-products. Cem Concr Res. 2004;34:1243-9.
[9] Sabir BB, Wild S, Bai J. Metakaolin and cacined clays as Pozzolans for concrete: A review. Cem Concr Compos. 2001;23:441-54.
[10] Changling H, Osbaeck B, Makovicky E. Pozzolanic reaction of six principal clay minerals: activation reactivity assessments and technological effects. Cem Concr Res. 1995;25:1691-702.
[11] Badogiannis E, Tsivilis S. Exploitation of poor Greek kaolins: Durability of metakaolin concrete. Cem Concr Compos. 2009; 31:128-33.
[12] Coleman NJ, Page CL. Aspects of the pore solution chemistry of hydrated cement pastes containing MK. Cem Concr Res. 1997;27:147-54.
[13] Zhang MH, Malhotra VM. Characteristics of a thermally activated aluminosilicate pozzolanic material and its use in concrete. Cem Concr Res. 1995;25:1713-25.
[14] Curcio F, DeAngelis BA. Dilatant behaviour of superplasticized cement pastes containing metakaolin. Cem Concr Res. 1998; 28:629-34.
[15] Shekarchi M, Bonakdar A, Bakhshi M, Mirdamadi A, Mobasher B. Transport properties in metakaolin blended concrete. Constr Build Mater. 2010;24:2217-23.
[16] Ramezanianpour AA, Pilvar A, Mahdikhani M, Moodi F. Practical evaluation of relationship between concrete resistivity, water penetration, rapid chloride penetration and compressive strength. Constr Build Mater. 2011;25: 2472-9.
[17] ASTM C1202-12. Standard test method for electrical indication of concrete's ability to resist chloride ion penetration. Philadelphia: American Society for Testing and Materials; 2002.
[18] ASTM C666A. Standard test method for characterizing air voids systems in Portland cement pervious concrete. Philadelphia: American Society for Testing and Materials; 2002.